STAT1/MUC4 activation promotes antimicrobial peptide production to reduce intestinal epithelium barrier injury caused by enteropathogenic Escherichia coli infection

Keywords
ZO-1, antimicrobial peptide, enteropathogenic Escherichia coli infection, intestinal epithelium barrier injury, STAT1/MUC4 pathway

Abstract

Introduction
Antimicrobial peptides (AMPs) are endogenous peptides that have been identified to alleviate intestinal epithelial barrier inflammation and dysfunction caused by enteropathogenic Escherichia coli (EPEC) infection; nonetheless, the upstream molecular mechanism of the production of AMPs is poorly understood.

Material and methods
The binding of signal transducer and activator of transcription (STAT) 1 (STAT1) to mucin 4 (MUC4) was examined by Co-Immunoprecipitation assay. To detect the influence of STAT1 and MUC4 expression, C57BL/6 mice model of EPEC infection in vivo and EPEC infected intestinal epithelial cells (IEC) in vitro model was established. Expressions of STAT1, MUC4, phosphorylated (p)-STAT1, proinflammatory cytokines, zonula occludens-1 (ZO-1) and AMP-related genes in mouse ileum and/or IEC were analyzed by immunohistochemical test, immunofluorescence assay, Western blot, and/or qRT-PCR. Meanwhile, IEC viability and apoptosis were measured using CCK-8 assay and flow cytometry.

Results
p-STAT1, MUC4, ZO-1 and AMP-related gene were lowly expressed in the ileum of EPEC-infected mice. p-STAT1 and MUC4 bound to each other. The expressions of STAT1 and MUC4 were decreased in EPEC-infected IEC. Overexpression of STAT1 resisted EPEC-induced viability decrease, apoptosis promotion, ZO-1 activity inhibition, release of proinflammatory cytokines, and downregulation of MUC4 and AMP-related genes in IEC. MUC4 knockdown partly counteracted the effect of STAT1 overexpression, but did not affect the forced STAT1 overexpression in EPEC-infected IEC.

Conclusions
STAT1/MUC4 pathway activation promotes AMP production to mitigate intestinal epithelium barrier injury caused by EPEC infection.

STAT1/MUC4 activation promotes antimicrobial peptide production to reduce intestinal epithelium barrier injury caused by enteropathogenic *Escherichia coli* infection

Running title: Effects of STAT1/MUC4 on gut EPEC infection

Liu Pei[1]*, Zhigang Zuo[2]*, Meixiang Zhang[2], Likun Zhao[2], Kaishuang Li[2]

[1]Department of Laboratory, The First Hospital of Qinhuangdao

[2]Department of Critical Care Medicine, The First Hospital of Qinhuangdao

*These authors contributed equally to this work.

Corresponding author: Zhigang Zuo, Department of Critical Care Medicine, The First Hospital of Qinhuangdao, No.258 Wenhua Road, Haigang District, Qinhuangdao City, Hebei Province, China

E-mail: zuozhigang_zzg@163.com

Abstract

Introduction: Antimicrobial peptides (AMPs) are endogenous peptides that have been identified to alleviate intestinal epithelial barrier inflammation and dysfunction caused by enteropathogenic *Escherichia coli* (EPEC) infection; nonetheless, the upstream molecular mechanism of the production of AMPs is poorly understood.

Material and methods: The binding of signal transducer and activator of transcription (STAT) 1 (STAT1) to mucin 4 (MUC4) was examined by Co-Immunoprecipitation assay. To detect the influence of STAT1 and MUC4 expression, C57BL/6 mice model of EPEC infection *in vivo* and EPEC infected intestinal epithelial cells (IEC) in *vitro* model was established. Expressions of STAT1, MUC4, phosphorylated (p)-STAT1, proinflammatory cytokines, zonula occludens-1 (ZO-1) and AMP-related genes in mouse ileum and/or IEC were analyzed by immunohistochemical test, immunofluorescence assay, Western blot, and/or qRT-PCR. Meanwhile, IEC viability and apoptosis were measured using CCK-8 assay and flow cytometry.

Results: p-STAT1, MUC4, ZO-1 and AMP-related gene were lowly expressed in the ileum of EPEC-infected mice. p-STAT1 and MUC4 bound to each other. The expressions of STAT1 and MUC4 were decreased in EPEC-infected IEC. Overexpression of STAT1 resisted EPEC-induced viability decrease, apoptosis promotion, ZO-1 activity inhibition, release of proinflammatory cytokines, and downregulation of MUC4 and AMP-related genes in IEC. MUC4 knockdown partly counteracted the effect of STAT1 overexpression, but did not affect the forced STAT1

overexpression in EPEC-infected IEC.

Conclusion: STAT1/MUC4 pathway activation promotes AMP production to mitigate intestinal epithelium barrier injury caused by EPEC infection.

Keywords: antimicrobial peptide, enteropathogenic *Escherichia coli* infection, intestinal epithelium barrier injury, STAT1/MUC4 pathway, ZO-1

Introduction

Escherichia coli (*E. coli*) is a Gram-negative rod-shaped bacterium that has a commensal relation with human without exerting any adverse effects [21]. However, commensal *E. coli* can be pathogenic, once it transforms into *pathovars* like Enteropathogenic *Escherichia coli* (EPEC), whose inhabitation on the gastrointestinal (GI) tract causes diarrheagenic and extraintestinal diseases in humans [47]. Besides, EPEC usually present in the food and water, therefore is also known as food-borne pathogens [24]. EPEC infection also induces malnutrition, which further increases the severity of the diseases caused by EPEC [22; 25]. It has been reported that EPEC infection is linked with remarkable morbidity and mortality of people with diarrhea in developing countries [33].

The pathogenic mechanism of EPEC involves interaction with enterocytes to form attaching and effacing (A/E) lesions that give rise to destruction of the microvilli, formation of actin pedestal, and reorganization of cytoskeleton, followed by reduction of epithelial barrier area [18; 65]. Tight junctions, which reside at the apical part of

the lateral membrane of intestinal epithelial barrier, are assembled by cytoplasmic scaffolding proteins like zonula occludens-1 (ZO-1), a scaffolding membrane protein [56]. Tight junctions serve to connect intestinal epithelial cells, maintain barrier polarity and regulate barrier function [46; 57]. Redistribution of tight junctions can be caused by EPEC-induced epithelial inflammation [17; 69], leading to altered barrier function.

Antimicrobial peptides (AMPs) are highly diverse and dynamic anti-infective molecules expressed by specific intestinal epithelial cells, paneth cells, and immune cells in the GI tract [5; 45]. AMPs also could target virulence protein [31]. Previous study showed that Human α-defense in 5 (HD5), which is the most abundant pan cell AMPs, and its treatment of *E. coli* can cause blister morphology, which is associated with cell death [16]. Besides, AMPs exhibit activity against a broad spectrum of bacteria through either affecting membrane stability or interfering with DNA replication, transcription, translation, protein biosynthesis, protein folding, or cell division [6; 20; 35]. Moreover, AMPs function as host immune response-modulating peptides to regulate gut microbial growth and composition [53]. Reduction of intestinal AMPs is associated with enteric dysbiosis and damage [67]. Research has shown that AMPs exert therapeutic effects against intestinal epithelial barrier inflammation and dysfunction caused by EPEC infection [2]. However, the upstream mechanism of the therapeutic effects has yet to be uncovered.

Previous study indicated that MUC4 deletion resulted in significant down-regulation of these AMPs at the mRNA level [54]. And stimulation of signal

transducer and activator of transcription (STAT) 1 (STAT1) expression can induce MUC4 expression [3]. And downregulation of STAT-1 has been recorded to be accompanied by a reduction in AMP formation, leading to intestinal microenvironmental disorders [67]. STAT1 is a member of intestinal STATs, which are a class of transcription factors crucial for transmitting intracellular signaling involved in cellular growth, differentiation, apoptosis, inflammation and immune responses [19; 42]. Evidence has indicated that STATs play essential roles in modulating the antimicrobial responses [38; 58]. Deficiency of STAT1 increases the susceptibility of mice to infection caused by microbial bacterial pathogens and viruses [41]. In addition, STAT1 has been documented to positively regulate the expression of mucin 4 (MUC4) by acting as a transcription factor of MUC4 [32]. MUC4 belongs to the transmembrane mucin family, whose secretion fends off microorganisms [43]. MUC4 is normally expressed in epithelia of several organs including colon [4], where it can protect the apical surfaces of epithelial cells [10]. Besides, MUC4 acts as an intramembrane ligand that modulates epithelial cell proliferation or differentiation after binding to ErbB2 [11]. Notably, knockout of MUC4 causes a less distribution of AMPs in mice bearing colorectal cancer (CRC) [54]. Taken together, it is assumed that STAT1 upregulates MUC4 level to induce AMP formation and thereby alleviate intestinal epithelial barrier injury caused by EPEC.

To test the assumption, the expressions of and interaction between STAT1 and MUC4 were examined using *in vivo* models of EPEC-induced intestinal infections, and the related *in vitro* models were established to confirm the role of the

STAT1/MUC4 pathway in EPEC-caused intestinal epithelial barrier injury.

Methods and materials

Ethics statement

All animal experiment procedures were performed in strict accordance with the guidelines of the National Institutes of Health on Animal Care and Use, and has been approved by the Ethics Committee of Qinhuangdao First Hospital (approval number:2022k015).

Animals

Male C57BL/6 mice (n=18, aged 22 days, weighing 10-12 g) were housed in animal cages at 22 ± 1.0 °C, in 50 ± 5% humidity, with a 14-hour (h) light and 10-h dark circadian cycle. Standard rodent house chow diet was given to the mice from their arrival through the infection.

Preparation and culture of EPEC inocula

The bacterial strain used in the present study was EPEC E2348/69 (serotype O127:H6), which belongs to phylogroup B2 with its full-length chromosomal nucleotide accessible by the Accession number: FM180568 [30]. Culture of EPEC was conducted in Dulbecco's modified Eagle's medium (DMEM; 11965092, ThermoFisher, Waltham, MA, USA) at 37°C in a shaking incubator, and was terminated when the EPEC cultures turned orange indicating optimal growth, with optical density $(OD)_{600}$~0.6. The EPEC cultures underwent centrifugation at 3500 × g for 10 minutes (min) at 4°C to obtain bacterial pellets, which were then resuspended in DMEM to reach a density of 10^{10} CFU/mL [36].

Establishment of mouse models of EPEC infection

Mice were given drinking water containing an antibiotic cocktail (35 mg/L gentamicin (A1720, Sigma-Aldrich, St. Louis, MO, USA), 45 mg/L vancomycin (SBR00001, Sigma-Aldrich, USA), 215 mg/L metronidazole (M1547, Sigma-Aldrich, USA), and 0.085 mg/L colistin (HY-113678, MedChemExpress, Monmouth Junction, NJ, USA) for 3 days to disrupt resident microbiota, the mice showed hunching posture and diarrhea. Then, the antibiotics were cleared by drinking normal water for 1 day, after which infection with EPEC was carried out [7]. In brief, mice were randomized into two groups. Those (n=6) in EPEC group were orally challenged with 100 μL of DMEM containing 10^{10} CFU/mL EPEC via a 22-gauge feeding needle [36], while control mice (n=6) were administrated with 100 μL DMEM instead.

Three days after the infection [36], all the mice were anesthetized by 1% pentobarbital sodium (P010, 50 mg/kg, Sigma-Aldrich, USA) and sacrificed via decapitation. Mouse ileum was collected and used for molecular assays.

Immunohistochemical test

Mouse ileum was fixed by 4% paraformaldehyde (P885233, MACKLIN, Shanghai, China) for 24 h, followed by treatment with gradient ethanol and xylene (95682, Sigma-Aldrich, USA). Then, the ileum was paraffinized (1496904, Sigma-Aldrich, USA) and cut into 4-μm-thick slices using a cryomicrotome (Leica CM 1850 UV, Leic Biosystems, Nussloch GmbH, Germany). After being deparaffinized, the slices were rehydrated and then water-boiled at 95℃ with repair solution (P0088, Beyotime, Shanghai, China) for 10 min to repair antigen. Later,

endogenous peroxidases were eliminated by the 10-min treatment with 3% H_2O_2, following which the slices were blocked in 5% bovine serum albumin (BSA; B928042, MACKLIN, China) for 30 min at 37℃. Thereafter, the slices were incubated with primary antibody for phosphorated (p)-STAT1 (ab109461, Abcam, Cambridge, UK) at 4℃ overnight, and with HRP-conjugated goat anti-rabbit IgG secondary antibody (31460, ThermoFisher, USA) for 1 h in the dark. Areas positive for p-STAT1 were visualized by the addition of DAB solution (D8001, Sigma-Aldrich, USA). Counterstaining was conducted with hematoxylin (H9627, Sigma-Aldrich, USA). Staining results were observed via an optical microscope (CX31-LV320, Olympus, Tokyo, Japan) under 100 × magnification.

Co-Immunoprecipitation (Co-IP) assay

Fresh mouse ileum from infected and control mice was homogenized and treated with T-PER histone protein extraction reagent (78510, ThermoFisher, USA) to isolate protein lysate, where the interaction between p-STAT1 and MUC4 was verified using Pierce Co-Immunoprecipitation kits (26149, ThermoFisher, USA). In short, the isolated lysate was precleared by Agarose Resin, and then incubated overnight at 4℃ with Agarose Resin coupled with normal Rabbit IgG (ab171870, Abcam, UK) or antibody for p-STAT1 (ab109461, Abcam, UK) or MUC4 (PA5-23077, ThermoFisher, USA). Later, immunocomplexes were generated. After being eluted using elution buffer (21009, ThermoFisher, USA), the immunocomplexes were subjected to Western blot, by which the enrichment of p-STAT1 or MUC4 was examined.

Western blot

Total protein was isolated from fresh mouse ileum by using RIPA Lysis Buffer supplemented with protease and phosphatase inhibitors (PPC1010, Sigma-Aldrich, USA). After being quantitated using a BCA kit (A53227, ThermoFisher, USA), the isolated proteins (30 μg) were denatured at 98°C for 10 min, and separated on 6% and 8% SDS-PAGE gel (P0686/P0688, Beyotime, China). The separated proteins were transferred onto a polyvinylidene fluoride (PVDF) membrane (1620256, BIO-RAD, Hercules, CA, USA), and then blocked in 5% BSA for 1 h at room temperature. Following wash with TBS-T (ab64204, Abcam, UK) thrice, the membrane was incubated with primary antibodies for p-STAT1 (ab109461, 89 kDa, 1:1000, Abcam, UK), MUC4 (PA5-23077, 71 kDa, 1:5000, ThermoFisher, USA) and GAPDH (ab8245, 37 kDa, 1:500, Abcam, UK) overnight at 4℃ under gentle agitation. Later, the membrane was washed with TBS-T, followed by incubation with Goat anti-Rabbit/Mouse IgG secondary antibodies (ab97051/ab6728, Abcam, UK) for 2 h at room temperature. Protein bands were developed with Clarity™ Western ECL Substrate (1705060, BIO-RAD, USA) on an imaging system (LAS-3000, Fujifilm, Tokyo, Japan), and the band intensity was quantified using ImageJ software (3.0 version, National Institutes of Health, Bethesda, MA, USA).

Cell isolation, culture and transfection

Primary mouse intestinal epithelial cells (IECs) were isolated from healthy male C57BL/6 mice (n=6) as previously described [48]. Simply put, mouse small intestines were dissected and washed by a solution containing 0.154 M NaCl and 1mM DTT. Intestinal segments were incubated with phosphate buffered saline (PBS; P5493,

Sigma-Aldrich, USA) at 37°C for 15 min. Then, the PBS used for incubation was added with 1.5 mM EDTA (EDS, Sigma-Aldrich, USA) and 0.5 mM DTT, and incubated with the segments for an additional 30 min, followed by the obtainment of IECs.

The isolated IECs were grown in DMEM (11966025, ThermoFisher, USA) supplemented with 10% fetal bovine serum (FBS; 12484028, ThermoFisher, USA) and penicillin-streptomycin (15140122, 100 U/mL-100 μg/mL, ThermoFisher, USA) in fibronectin-coated plates at 37°C with 5% CO_2.

STAT1 overexpression plasmids were synthesized using pcDNA™3.1 (V79020, ThermoFisher, USA), with empty vectors serving as the negative control (NC). pLKO.1-puro vectors (SHC016, Sigma-Aldrich, USA) were utilized to produce short harpin RNA against MUC4 (shMUC4) (sense, 5'-UAUUAAUCUCUUAUCUUCCAC-3'; antisense, 5'-GGAAGAUAAGAGAUUAAUAGG-3'), and the negative control (shNC) of shMUC4 was set using empty pLKO.1-puro vectors. IECs were transfected with NC plus shNC or STAT1 overexpression plasmids plus shNC/shMUC4, with the aid of Lipofectamine 3000 transfection reagent (L3000015, ThermoFisher, USA). Briefly, IECs were inoculated in 96-well plates at a density of 1×10^4 cells/well until the confluency of cells reached 80%. After dilution together with Opti-MEM and P3000 reagent, the plasmids and Lipofectamine 3000 transfection reagent were incubated together for 15 min at 37°C to generate gene-lipid complexes, which were later incubated with the cells for 48 h for transfection.

Cell infection

IECs seeded in 96-well plates were grown to become an 80% confluent monolayer, and then challenged with 1×10^6 CFU/well EPEC for 1 h or 2.5 h (only for flow cytometry) at 37°C [23].

Cell counting kit (CCK)-8 assay

Transfected IECs were implanted in 96-well plates and challenged with EPEC. Then, after the cells were adherent to the plate, 10 μL CCK-8 reagent (CA1210, Solarbio, Beijing, China) was added into each well, and incubated with cells for 2 h at 37℃. The OD of each well was read at 450 nm by a microplate reader (EMax Plus, Molecular Devices, Sunnyvale, CA, USA), and relative cell viability was calculated according to the formula: Cell viability (%) $=(OD_{\text{treatment group}}-OD_{\text{blank group}})/(OD_{\text{control group}}-OD_{\text{blank group}}) \times 100$.

Flow cytometry

Transfected IECs were subjected to apoptosis assay performed with AnnexinV-FITC/PI Staining kits (ab14085, Abcam, UK). In brief, the cells were challenged with EPEC, and then digested for 10 min with 0.25% EDTA-free trypsin (T6325, MACKLIN, China). Centrifugation at 2000 × g was conducted for 10 min to obtain 1×10^5 cells. After being flushed with PBS, the cells were resuspended in Annexin V binding buffer, and then added with Annexin V-FITC (5 μL) and propidium iodide (PI) (5 μL). Cell incubation was performed for 5 min protected from light at room temperature. The cells were later transferred onto a flow cytometer (Cytoflex, Beckman Coulter, Brea, CA, USA) for apoptosis detection, and data

analysis was implemented using FlowJo software (Tree Star, Ashland, OR, USA).

Immunofluorescence assay

The deparaffinized mouse ileum slices from immunohistochemical test were dehydrated and received antigen repair. Transfected IECs were infected, fixated in 4% paraformaldehyde for 15 min, and permeabilized using 0.3% Triton X-100 (X100, Sigma-Aldrich, USA) for 20 min. Both the slices and the cells were blocked in 5% BSA for 30 min at room temperature, and incubated at 4℃ overnight with antibodies for MUC4 (PA5-23077, Rabbit, ThermoFisher, USA) and ZO-1 (for tissues, 14-9776-82, Rat, ThermoFisher, USA)/(for cells, 40-2200, Rabbit, ThermoFisher, USA). Later, they were probed with secondary antibodies, Goat anti-Rabbit IgG (H+L) conjugated with Alexa Fluor™ 488 (A-11008, ThermoFisher, USA) and Goat anti-Rat IgG (H+L) conjugated with Alexa Fluor™ 594 (A-11007, ThermoFisher, USA), and then counterstained with DAPI (D9542, Sigma-Aldrich, USA). Images were developed using a confocal scanning microscope (ECLIPSE TI-SR, Nikon, Japan)

Quantitative reverse transcription polymerase chain reaction (qRT-PCR)

Total RNA was extracted from fresh mouse ileum as well as IECs using Trizol reagents (15596026, ThermoFisher, USA), and then the total RNA concentration was determined using a spectrophotometer (NanoDrop 2000, ThermoFisher, USA). cDNA was generated utilizing reverse transcription kits (K1622, Yaanda Biotechnology, Beijing, China). Next, cDNA was amplified on a PCR detection system (LightCycler 96, Roche, Indianapolis, IN, USA) with Eastep qPCR Master Mix (LS2062, Promega, Madison, WI, USA), with the primers listed in Table 1, under the following

thermocycle: 40 circles of 95°C for 10 min, 95°C for 15 seconds (s) and 60°C for 1 min. Gene expressions relative to the expression of housekeeping gene GAPDH were calculated using the $2^{-\Delta\Delta Ct}$ method [39].

Statistical analysis

A total of 18 Male C57BL/6 mice were included in these experiments. Statistical analysis was conducted on a sample size of 6 for EPEC-infected mice, 6 for control mice. And the remaining 6 Male C57BL/6 mice were used to isolate IECs, which were used for subsequent experiments, and three parallel experiments were set up for each group. Graphpad prism (version 8.0, GraphPad Software Inc., San Diego, CA, USA) was exploited for statistical analysis. All data were described by mean ± standard deviation (SD) from experiments repeated at least three. Comparison between two groups was implemented via independent-*t* test, while that among multiple groups was carried out using one-way analysis of variance (ANOVA). A difference was considered statistically significant when $P<0.05$.

Results

p-STAT1, MUC4, ZO-1 and AMP-related gene were lowly expressed in the ileum of EPEC-infected mice.

STAT1 downregulation has been reported to be concomitant with a reduction in AMP formation, resulting in intestinal microenvironmental disorders [67]. Moreover, AMPs are less distributed in mice bearing CRC as a result of MUC4 knockout [54]. We first investigated the expression of p-STAT1 and MUC4 in mouse EPEC model. Immunohistochemical test results showed that in the ileum of EPEC-infected mice,

p-STAT1 expression declined considerably (Fig. 1A). MUC4 was found to be lowly expressed in the ileum of EPEC-infected mice through immunofluorescence assay (Fig. 1B). Besides, we also found that this was accompanied by a decreased expression of ZO-1 (Fig. 1C). Further, Western blot analysis reaffirmed that the expressions of p-STAT1 and MUC4 both diminished in the ileum of EPEC-infected mice (Fig. 2A, P <0.001). Then, to determine how AMP level is affected in EPEC-induced intestinal infection, AMP-related gene expressions were analyzed by qRT-PCR, the results of which revealed that the expressions of Defa1, Defa4, Defa5, Camp and Lyz1 all diminished in the ileum of mice after EPEC infection (Fig. 2B-F, P <0.001). In conclusion, we verified that the expression levels of p-STAT1, MUC4, ZO-1 and AMP-related gene were lower in the EPEC-infected mice. And STAT1 can positively regulate MUC4 expression [32]. Therefore we next explored STAT1 and MUC4 could interact.

Co-IP assay was then performed to investigate the interaction between p-STAT1 and MUC4, and the results proved that antibodies for p-STAT1 enriched MUC4 proteins and antibodies for MUC4 enriched p-STAT1 proteins in the ileum of both control and EPEC-infected mice (Fig. 2G). This indicated that p-STAT1 and MUC4 can interact with each other. Then, through *in vitro* experiments, we explored the STAT1/MUC4 pathway on IECs viability, apoptosis and related inflammatory factors.

STAT1/MUC4 pathway was downregulated in EPEC-induced IECs and its forced upregulation resisted EPEC-induced IEC viability decreases.

IECs were infected with EPEC to establish *in-vitro* intestinal infections, where

the role of the STAT1/MUC4 pathway in EPEC-induced intestinal infections was examined. Transfection with STAT1 overexpression plasmids led to an increased expression of STAT1 (Fig. 3A, P <0.001), and MUC4 expression was knocked down by transfection with shMUC4 (Fig. 3B, P <0.001) in IECs. STAT1 expression declined with EPEC infection in IEC (Fig. 3C, P <0.001), which was reversed by STAT1 overexpression plasmid transfection (Fig. 3C, P <0.001). MUC4 knockdown had no obvious impact on the transfection-mediated STAT1 overexpression in EPEC-infected IECs (Fig. 3C). EPEC infection resulted in MUC4 downregulation in IECs (Fig. 3D, P <0.001). STAT1 overexpression abrogated EPEC infection-induced MUC4 downregulation (Fig. 3D, P <0.001), while such effect of STAT1 overexpression was attenuated by MUC4 knockdown (Fig. 3D, P <0.001). Moreover, decreased viability of IECs after EPEC infection was detected (Fig. 3E, P <0.001). STAT1 overexpression resisted the EPEC-induced IEC cell viability decrease (Fig. 3E, P <0.001); nevertheless, MUC4 knockdown mitigated the promotive effect of STAT1 overexpression on the viability of EPEC-infected IECs (Fig. 3E, P <0.05).

Forced upregulation of STAT1/MUC4 pathway offset EPEC-induced apoptosis promotion and release of proinflammatory cytokines in IEC.

Subsequently, EPEC infection was observed to induce apoptosis of IECs (Fig. 4A-B, P <0.001), which was offset by STAT1 overexpression (Fig. 4A-B, P <0.001). MUC4 knockdown attenuated the inhibiting effect of STAT1 overexpression on apoptosis of EPEC-infected IECs (Fig. 4A-B, P <0.001). In addition, the levels of proinflammatory cytokines (IL-1, TNF-α and IL-6) rose in IEC following EPEC

infection (Fig. 4C-E, P <0.001). STAT1 overexpression caused downregulation of IL-1, TNF-α and IL-6 in EPEC-infected IECs (Fig. 4C-E, P <0.001), but the downregulation was mitigated by MUC4 knockdown (Fig. 4C-E, P <0.05).

Forced upregulation of STAT1/MUC4 pathway resisted EPEC-induced ZO-1 downregulation in IEC.

Through immunofluorescence assay, the expression of ZO-1 was detected to be reduced by EPEC infection in IEC, and this ZO-1 expression reduction can be abrogated by STAT1 overexpression (Fig. 5). MUC4 knockdown weakened the effect of STAT1 overexpression on ZO-1 expression in EPEC-infected IECs through suppressing ZO-1-postive fluorescence (Fig. 5).

Forced upregulation of STAT1/MUC4 pathway reversed EPEC-induced AMP-related gene downregulation in IEC.

Finally, whether and how the STAT1/MUC4 pathway influences AMP formation in *in-vitro* intestinal infection were investigated. Upon EPEC infection, the expressions of AMP-related genes (Defa1, Defa4, Defa5, Camp and Lyz1) all decreased in IECs (Fig. 6A-E, P <0.001). STAT1 overexpression observably upregulated the expressions of these AMP-related genes, and reversed the EPEC-induced negative effect on AMP formation in IECs (Fig. 6A-E, P <0.001). However, MUC4 knockdown offset the STAT1 overexpression-induced upregulation of these AMP-related genes in EPEC-infected IECs (Fig. 6A-E, P <0.01).

Discussion

EPEC infection remains a public health concern in developing countries, leading

to diarrheal diseases with a risk of death [52]. AMPs can act as endogenous antibiotics to direct bactericidal activity, thereby reducing epithelial barrier injury caused by EPEC infection [8]. In the present study, the STAT1/MUC4 pathway is identified as the upstream mechanism of AMP-induced protection against EPEC infection in intestinal epithelial barriers.

Inhibited STAT1 signaling is associated with the exacerbation of enteropathogenic bacterial infection-caused intestinal hyperplasia and diarrhea in mice [64]. In mouse models of chronic alcohol-induced intestinal injury, lack of p-STAT1 and of total STAT1 in the ileum cooccurs with downregulation of small intestinal AMPs, resulting in disrupted gut microbiota homeostasis [67]. The above findings suggested that STAT1 downregulation or inactivation may be connected with microbiota homeostasis disruption following bacterial infection. Consistently, our study displayed that STAT1 phosphorylation diminished in the ileum of mice following EPEC infection. In contrast, Ceponis et al. demonstrated that EPEC infection in epithelial cells could not eliminate STAT1 tyrosine phosphorylation induced by IFN-gamma [12]. However, EPEC exhibits considerable genomic diversity, being represented in at least 10 different phylogenomic lineages [26], so EPEC with different phenotypes may have different effects. In our study, STAT1 mRNA level declined in IEC after EPEC infection, which, together with Ceponis's results, implies that EPEC infection reduces STAT1 mRNA expression but is unable to affect STAT1 phosphorylation. Therefore, the decrease of STAT1 phosphorylation in the ileum of mice following EPEC infection may be attributed to the decreased

level of STAT1 designated to undergo phosphorylation. This also justifies the discrepancy between our and Ceponis's results. Further, IFN-gamma, which can elicit STAT1 activation, is an important cytokine against infection by viral and microbial pathogens in host defense [61], and is induced in mice and human following EPEC injection [27; 62]. EPEC burden is higher in immunocompromised patients than in healthy adults [50]. These suggested that in healthy adults, host defense is activated to upregulate IFN-gamma, which activates STAT1 and thus prevents EPEC infection.

The attachment of EPEC on the epithelium disrupts normal cellular process [14]. EPEC encodes a subset of effectors that induce apoptosis of epithelial cells to cause cell death and barrier dysfunction [49; 60]. Moreover, inflammation of the intestinal mucosa occurs after EPEC infection, where EPEC is involved in stimulation of the proinflammatory cytokine TNF-α production to promote myosin light chain (MLC) phosphorylation, thereby making contribution to barrier dysfunction [59; 65]. Also, following EPEC infection, rabbit enterocytes and rat colonic mucosa scrapings have been discovered to exhibit upregulated proinflammatory cytokines, IL-1β and IL-6 [1; 55], whose release is mediated by TNF-α [40]. In our study, we overexpressed STAT1 in order to achieve prominent STAT1 activation in IECs, and found that EPEC-induced apoptosis and upregulation of TNF-α, IL-1β and IL-6 were weakened by STAT1 overexpression.

Epithelial barrier dysfunction manifests alteration of tight junctions [65], which act as the barrier required to maintain polarity that aids the directional diffusion of solutes [63]. ZO-1 is a cytoplasmic scaffolding protein that constitutes tight junctions

along with other membrane proteins [51], and plays a dispensable role for barrier function [34]. In our study, low ZO-1 expression caused by EPEC infection was reversed by STAT1 overexpression in IECs. The above results collectively indicated that STAT1 overexpression mitigated EPEC-induced intestinal epithelial barrier dysfunction.

In addition, paneth cells are specialized cells in the intestinal epithelium [5], who assist the intestinal mucosa to maintain the functional intestinal epithelial barrier by secreting AMPs to modulate innate immunity [29], or directly kill their target bacteria [68]. Our study showed that in the ileum of mice and IECs following EPEC infection, p-STAT1 and STAT1 downregulation was concomitant with reduction of AMP formation, as reflected by decreased levels of AMP-related genes (Defa1, Defa4, Defa5, Camp and Lyz1), which is in line with their status in alcohol-induced intestinal injury [67]. Moreover, we observed that STAT1 overexpression facilitated AMP formation. AMPs are considered as therapeutic agents for treating infections caused by untreatable microorganisms. According to this and our results above, STAT1 activation is presumed to prevent EPEC infection by facilitating AMP formation.

The expression of MUC4, a member of transmembrane mucin family, increases along with decreased epithelial paracellular permeability [37]. STAT1 can transcriptionally upregulate MUC4 level [32], which is reaffirmed in our study. Besides, MUC4 protects epithelial surfaces against infections and injury [13]. MUC4 is lowly expressed in intestinal epithelial cells from patients with inflammatory bowel disease [9]. Notably, knockout of MUC4 leads to less AMP formation in CRC mice

[54]. Our study revealed that MUC4 level decreased with STAT1 phosphorylation inhibited in the ileum of mice and IECs after EPEC infection, and MUC4 knockdown offset the effects of STAT1 overexpression on apoptosis, inflammation, and AMP formation in EPEC-infected IEC.

Previous study also proved that JAK/STAT-1 plays a critical role in the regulation of uropathogenic *E. coli* invasion [15; 28]. Besides, the oral antimicrobial peptide Mastoparan X alleviates intestinal inflammation caused by enterohemorrhagic *E. coli* and regulates the gut microbiota [70]. Besides, *E. coli* also is an important cause of spontaneous bacterial peritonitis (SBP), which is one of the major complications of liver cirrhosis, which clinical symptoms include diarrhea, enhancing intestinal barrier function is a novel strategy for the treatment of cirrhosis, as impaired intestinal barrier function can lead to translocation of intestinal bacteria [44]. Therefore, further studies are required to determine whether the mechanism of STAT1/MUC4 activation promotes antimicrobial peptide production to reduce intestinal epithelium barrier injury may emerge in other types of diarrhea-induced microorganism. Besides, noncommunicable diarrhea can be caused by toxins, chronic diseases, or antibiotics [66]. Whether this mechanism also exists in non-infectious diarrhea needs further study.

There are some limitations in this study. EPEC may change the intestinal flora, and we did not study the effects of STAT1/MUC4 on the microbiota, which would be study in the future. In addition, whether STAT1/MUC4 affects intestinal epithelium barrier injury will cause translocation of microorganisms needs further research.

Conclusion

The present study demonstrated that the STAT1/MUC4 pathway is downregulated in intestinal epithelium after EPEC infection, and its activation facilitates AMP formation, partaking in the prevention of EPEC-induced intestinal epithelium infection.

Acknowledgements

Not applicable

Funding

No funding was received for this research.

Disclosure of Conflict-of-Interest

I, as the corresponding author, declare, on behalf of all authors of the paper, that no financial conflict of interest exists in relation to the work described.

Availability of Data and Materials

The analyzed data sets generated during the study are available from the corresponding author on reasonable request.

References

1. Abdallah Hajj Hussein, I., Freund, J. N., Reimund, J. M., et al., 2012. Enteropathogenic e.coli sustains iodoacetamide-induced ulcerative colitis-like colitis

in rats: modulation of IL-1β, IL-6, TNF-α, COX-2, and apoptosisi. Journal of biological regulators and homeostatic agents 26, 515-526.

2. Al-Mamun, A., Mily, A., Sarker, P., et al., 2013. Treatment with phenylbutyrate in a pre-clinical trial reduces diarrhea due to enteropathogenic Escherichia coli: link to cathelicidin induction. Microbes and infection 15, 939-950.

3. Andrianifahanana, M., Singh, A. P., Nemos, C., et al., 2007. IFN-gamma-induced expression of MUC4 in pancreatic cancer cells is mediated by STAT-1 upregulation: a novel mechanism for IFN-gamma response. Oncogene 26, 7251-7261.

4. Audie, J. P., Janin, A., Porchet, N., Copin, M. C., Gosselin, B., Aubert, J. P., 1993. Expression of human mucin genes in respiratory, digestive, and reproductive tracts ascertained by in situ hybridization. The journal of histochemistry and cytochemistry : official journal of the Histochemistry Society 41, 1479-1485.

5. Bevins, C. L., Salzman, N. H., 2011. Paneth cells, antimicrobial peptides and maintenance of intestinal homeostasis. Nature reviews. Microbiology 9, 356-368.

6. Bin Hafeez, A., Jiang, X., Bergen, P. J., Zhu, Y., 2021. Antimicrobial Peptides: An Update on Classifications and Databases. International journal of molecular sciences 22.

7. Bolick, D. T., Medeiros, P., Ledwaba, S. E., et al., 2018. Critical Role of Zinc in a New Murine Model of Enterotoxigenic Escherichia coli Diarrhea. Infection and immunity 86.

8. Brogden, K. A., 2005. Antimicrobial peptides: pore formers or metabolic inhibitors in bacteria? Nature reviews. Microbiology 3, 238-250.

9. Buisine, M. P., Desreumaux, P., Leteurtre, E., et al., 2001. Mucin gene expression in intestinal epithelial cells in Crohn's disease. Gut 49, 544-551.

10. Carraway, K. L., Perez, A., Idris, N., et al., 2002. Muc4/sialomucin complex, the intramembrane ErbB2 ligand, in cancer and epithelia: to protect and to survive. Progress in nucleic acid research and molecular biology 71, 149-185.

11. Carraway, K. L., Ramsauer, V. P., Haq, B., Carothers Carraway, C. A., 2003. Cell signaling through membrane mucins. BioEssays : news and reviews in molecular, cellular and developmental biology 25, 66-71.

12. Ceponis, P. J., McKay, D. M., Ching, J. C., Pereira, P., Sherman, P. M., 2003. Enterohemorrhagic Escherichia coli O157:H7 disrupts Stat1-mediated gamma interferon signal transduction in epithelial cells. Infection and immunity 71, 1396-1404.

13. Chaturvedi, P., Singh, A. P., Batra, S. K., 2008. Structure, evolution, and biology of the MUC4 mucin. FASEB journal : official publication of the Federation of American Societies for Experimental Biology 22, 966-981.

14. Chen, H. D., Frankel, G., 2005. Enteropathogenic Escherichia coli: unravelling pathogenesis. FEMS microbiology reviews 29, 83-98.

15. Chen, P. C., Ho, C. H., Fan, C. K., Liu, S. P., Cheng, P. C., 2022. Antimicrobial Peptide LCN2 Inhibited Uropathogenic Escherichia coli Infection in Bladder Cells in a High-Glucose Environment through JAK/STAT Signaling Pathway. International journal of molecular sciences 23.

16. Chileveru, H. R., Lim, S. A., Chairatana, P., Wommack, A. J., Chiang, I. L., Nolan,

E. M., 2015. Visualizing attack of Escherichia coli by the antimicrobial peptide human defensin 5. Biochemistry 54, 1767-1777.

17. Clayburgh, D. R., Barrett, T. A., Tang, Y., et al., 2005. Epithelial myosin light chain kinase-dependent barrier dysfunction mediates T cell activation-induced diarrhea in vivo. The Journal of clinical investigation 115, 2702-2715.

18. Croxen, M. A., Law, R. J., Scholz, R., Keeney, K. M., Wlodarska, M., Finlay, B. B., 2013. Recent advances in understanding enteric pathogenic Escherichia coli. Clinical microbiology reviews 26, 822-880.

19. Darnell, J. E., Jr., 1997. STATs and gene regulation. Science (New York, N.Y.) 277, 1630-1635.

20. Dubos, R. J., 1939. STUDIES ON A BACTERICIDAL AGENT EXTRACTED FROM A SOIL BACILLUS : I. PREPARATION OF THE AGENT. ITS ACTIVITY IN VITRO. The Journal of experimental medicine 70, 1-10.

21. Escobar-Páramo, P., Giudicelli, C., Parsot, C., Denamur, E., 2003. The evolutionary history of Shigella and enteroinvasive Escherichia coli revised. Journal of molecular evolution 57, 140-148.

22. Fagundes-Neto, U., Scaletsky, I. C., 2000. The gut at war: the consequences of enteropathogenic Escherichia coli infection as a factor of diarrhea and malnutrition. Sao Paulo medical journal = Revista paulista de medicina 118, 21-29.

23. Fu, Q., Lin, Q., Chen, D., et al., 2022. β-defensin 118 attenuates inflammation and injury of intestinal epithelial cells upon enterotoxigenic Escherichia coli challenge. BMC veterinary research 18, 142.

24. Govindarajan, D. K., Viswalingam, N., Meganathan, Y., Kandaswamy, K., 2020. Adherence patterns of Escherichia coli in the intestine and its role in pathogenesis. Medicine in Microecology 5, 100025.

25. Guerrant, R. L., Oriá, R. B., Moore, S. R., Oriá, M. O., Lima, A. A., 2008. Malnutrition as an enteric infectious disease with long-term effects on child development. Nutrition reviews 66, 487-505.

26. Hernandes, R. T., Hazen, T. H., Dos Santos, L. F., Richter, T. K. S., Michalski, J. M., Rasko, D. A., 2020. Comparative genomic analysis provides insight into the phylogeny and virulence of atypical enteropathogenic Escherichia coli strains from Brazil. PLoS neglected tropical diseases 14, e0008373.

27. Higgins, L. M., Frankel, G., Connerton, I., Gonçalves, N. S., Dougan, G., MacDonald, T. T., 1999. Role of bacterial intimin in colonic hyperplasia and inflammation. Science (New York, N.Y.) 285, 588-591.

28. Ho, C. H., Fan, C. K., Wu, C. C., et al., 2021. Enhanced uropathogenic Escherichia coli-induced infection in uroepithelial cells by sugar through TLR-4 and JAK/STAT1 signaling pathways. Journal of microbiology, immunology, and infection = Wei mian yu gan ran za zhi 54, 193-205.

29. Hooper, L. V., Macpherson, A. J., 2010. Immune adaptations that maintain homeostasis with the intestinal microbiota. Nature reviews. Immunology 10, 159-169.

30. Iguchi, A., Thomson, N. R., Ogura, Y., et al., 2009. Complete genome sequence and comparative genome analysis of enteropathogenic Escherichia coli O127:H6 strain E2348/69. Journal of bacteriology 191, 347-354.

31. Kandaswamy, K., Liew, T. H., Wang, C. Y., et al., 2013. Focal targeting by human β-defensin 2 disrupts localized virulence factor assembly sites in Enterococcus faecalis. Proceedings of the National Academy of Sciences of the United States of America 110, 20230-20235.

32. Kossow, C., Jose, D., Jaster, R., Wolkenhauer, O., Rateitschak, K., 2012. Mathematical modelling unravels regulatory mechanisms of interferon-γ-induced STAT1 serine-phosphorylation and MUC4 expression in pancreatic cancer cells. IET systems biology 6, 73-85.

33. Kotloff, K. L., Nataro, J. P., Blackwelder, W. C., et al., 2013. Burden and aetiology of diarrhoeal disease in infants and young children in developing countries (the Global Enteric Multicenter Study, GEMS): a prospective, case-control study. Lancet (London, England) 382, 209-222.

34. Kuo, W. T., Zuo, L., Odenwald, M. A., et al., 2021. The Tight Junction Protein ZO-1 Is Dispensable for Barrier Function but Critical for Effective Mucosal Repair. Gastroenterology 161, 1924-1939.

35. Le, C. F., Gudimella, R., Razali, R., Manikam, R., Sekaran, S. D., 2016. Transcriptome analysis of Streptococcus pneumoniae treated with the designed antimicrobial peptides, DM3. Scientific reports 6, 26828.

36. Ledwaba, S. E., Costa, D. V. S., Bolick, D. T., et al., 2020. Enteropathogenic Escherichia coli Infection Induces Diarrhea, Intestinal Damage, Metabolic Alterations, and Increased Intestinal Permeability in a Murine Model. Frontiers in cellular and infection microbiology 10, 595266.

37. Li, J., Zhang, L., Wu, T., Li, Y., Zhou, X., Ruan, Z., 2021. Indole-3-propionic Acid Improved the Intestinal Barrier by Enhancing Epithelial Barrier and Mucus Barrier. Journal of agricultural and food chemistry 69, 1487-1495.

38. Lieberman, L. A., Banica, M., Reiner, S. L., Hunter, C. A., 2004. STAT1 plays a critical role in the regulation of antimicrobial effector mechanisms, but not in the development of Th1-type responses during toxoplasmosis. Journal of immunology (Baltimore, Md. : 1950) 172, 457-463.

39. Livak, K. J., Schmittgen, T. D., 2001. Analysis of relative gene expression data using real-time quantitative PCR and the 2(-Delta Delta C(T)) Method. Methods (San Diego, Calif.) 25, 402-408.

40. Ma, K., Zhang, H., Baloch, Z., 2016. Pathogenetic and Therapeutic Applications of Tumor Necrosis Factor-α (TNF-α) in Major Depressive Disorder: A Systematic Review. International journal of molecular sciences 17.

41. Meraz, M. A., White, J. M., Sheehan, K. C., et al., 1996. Targeted disruption of the Stat1 gene in mice reveals unexpected physiologic specificity in the JAK-STAT signaling pathway. Cell 84, 431-442.

42. Mogensen, T. H., 2018. IRF and STAT Transcription Factors - From Basic Biology to Roles in Infection, Protective Immunity, and Primary Immunodeficiencies. Frontiers in immunology 9, 3047.

43. Moniaux, N., Escande, F., Porchet, N., Aubert, J. P., Batra, S. K., 2001. Structural organization and classification of the human mucin genes. Frontiers in bioscience : a journal and virtual library 6, D1192-1206.

44. Muñoz, L., Borrero, M. J., Úbeda, M., et al., 2019. Intestinal Immune Dysregulation Driven by Dysbiosis Promotes Barrier Disruption and Bacterial Translocation in Rats With Cirrhosis. Hepatology (Baltimore, Md.) 70, 925-938.

45. Muniz, L. R., Knosp, C., Yeretssian, G., 2012. Intestinal antimicrobial peptides during homeostasis, infection, and disease. Frontiers in immunology 3, 310.

46. Muza-Moons, M. M., Schneeberger, E. E., Hecht, G. A., 2004. Enteropathogenic Escherichia coli infection leads to appearance of aberrant tight junctions strands in the lateral membrane of intestinal epithelial cells. Cellular microbiology 6, 783-793.

47. Nash, J. H., Villegas, A., Kropinski, A. M., et al., 2010. Genome sequence of adherent-invasive Escherichia coli and comparative genomic analysis with other E. coli pathotypes. BMC genomics 11, 667.

48. Nenci, A., Becker, C., Wullaert, A., et al., 2007. Epithelial NEMO links innate immunity to chronic intestinal inflammation. Nature 446, 557-561.

49. Nougayrède, J. P., Donnenberg, M. S., 2004. Enteropathogenic Escherichia coli EspF is targeted to mitochondria and is required to initiate the mitochondrial death pathway. Cellular microbiology 6, 1097-1111.

50. Olvera, A., Carter, H., Rajan, A., et al., 2021. Enteropathogenic Escherichia coli Infection in Cancer and Immunosuppressed Patients. Clinical infectious diseases : an official publication of the Infectious Diseases Society of America 72, e620-e629.

51. Otani, T., Nguyen, T. P., Tokuda, S., et al., 2019. Claudins and JAM-A coordinately regulate tight junction formation and epithelial polarity. The Journal of cell biology 218, 3372-3396.

52. Pakbin, B., Brück, W. M., Rossen, J. W. A., 2021. Virulence Factors of Enteric Pathogenic Escherichia coli: A Review. International journal of molecular sciences 22.

53. Pasupuleti, M., Schmidtchen, A., Malmsten, M., 2012. Antimicrobial peptides: key components of the innate immune system. Critical reviews in biotechnology 32, 143-171.

54. Pothuraju, R., Pai, P., Chaudhary, S., et al., 2022. Depletion of transmembrane mucin 4 (Muc4) alters intestinal homeostasis in a genetically engineered mouse model of colorectal cancer. Aging 14, 2025-2046.

55. Ramirez, K., Huerta, R., Oswald, E., Garcia-Tovar, C., Hernandez, J. M., Navarro-Garcia, F., 2005. Role of EspA and intimin in expression of proinflammatory cytokines from enterocytes and lymphocytes by rabbit enteropathogenic Escherichia coli-infected rabbits. Infection and immunity 73, 103-113.

56. Rodgers, L. S., Beam, M. T., Anderson, J. M., Fanning, A. S., 2013. Epithelial barrier assembly requires coordinated activity of multiple domains of the tight junction protein ZO-1. Journal of cell science 126, 1565-1575.

57. Rose, E. C., Odle, J., Blikslager, A. T., Ziegler, A. L., 2021. Probiotics, Prebiotics and Epithelial Tight Junctions: A Promising Approach to Modulate Intestinal Barrier Function. International journal of molecular sciences 22.

58. Ruan, Z., Wan, Z., Yang, L., Li, W., Wang, Q., 2019. JAK/STAT signalling regulates antimicrobial activities in Eriocheir sinensis. Fish & shellfish immunology 84, 491-501.

59. Scott, K. G., Meddings, J. B., Kirk, D. R., Lees-Miller, S. P., Buret, A. G., 2002.

Intestinal infection with Giardia spp. reduces epithelial barrier function in a myosin light chain kinase-dependent fashion. Gastroenterology 123, 1179-1190.

60. Serapio-Palacios, A., Navarro-Garcia, F., 2016. EspC, an Autotransporter Protein Secreted by Enteropathogenic Escherichia coli, Causes Apoptosis and Necrosis through Caspase and Calpain Activation, Including Direct Procaspase-3 Cleavage. mBio 7.

61. Shtrichman, R., Samuel, C. E., 2001. The role of gamma interferon in antimicrobial immunity. Current opinion in microbiology 4, 251-259.

62. Tacket, C. O., Sztein, M. B., Losonsky, G., et al., 2000. Role of EspB in experimental human enteropathogenic Escherichia coli infection. Infection and immunity 68, 3689-3695.

63. Tsukita, S., Furuse, M., Itoh, M., 2001. Multifunctional strands in tight junctions. Nature reviews. Molecular cell biology 2, 285-293.

64. Tsutsuki, H., Zhang, T., Yahiro, K., et al., 2022. Subtilase cytotoxin from Shiga-toxigenic Escherichia coli impairs the inflammasome and exacerbates enteropathogenic bacterial infection. iScience 25, 104050.

65. Viswanathan, V. K., Hodges, K., Hecht, G., 2009. Enteric infection meets intestinal function: how bacterial pathogens cause diarrhoea. Nature reviews. Microbiology 7, 110-119.

66. Yu, J., Zhang, Y., Song, X., et al., 2017. Effect of Modified Pulsatilla Powder on Enterotoxigenic Escherichia coli O101-Induced Diarrhea in Mice. Evidence-based complementary and alternative medicine : eCAM 2017, 3687486.

67. Yue, R., Wei, X., Zhao, J., Zhou, Z., Zhong, W., 2020. Essential Role of IFN-γ in Regulating Gut Antimicrobial Peptides and Microbiota to Protect Against Alcohol-Induced Bacterial Translocation and Hepatic Inflammation in Mice. Frontiers in physiology 11, 629141.

68. Zasloff, M., 2002. Antimicrobial peptides of multicellular organisms. Nature 415, 389-395.

69. Zhang, Q., Li, Q., Wang, C., Li, N., Li, J., 2012. Redistribution of tight junction proteins during EPEC infection in vivo. Inflammation 35, 23-32.

70. Zhao, X. Q., Wang, L., Zhu, C. L., et al., 2022. Oral Administration of the Antimicrobial Peptide Mastoparan X Alleviates Enterohemorrhagic Escherichia coli-Induced Intestinal Inflammation and Regulates the Gut Microbiota. Probiotics and antimicrobial proteins.

FIGUER LEGENDS

Figure 1. p-STAT1, MUC4 and ZO-1 were lowly expressed in the ileum of EPEC-infected mice. (A/B/C). C57BL/6 mice were orally challenged with 100 μL of DMEM containing 10^{10} CFU/mL EPEC. (A). The expression of p-STAT1 in the ileum was detected by immunohistochemical test (magnification: × 100; scale bar: 50 μm). (B/C). The expressions of MUC4 and ZO-1 in the ileum were determined by immunofluorescence assay (magnification: × 400; scale bar: 50 μm). (n=6). (EPEC, enteropathogenic Escherichia coli; p-STAT1, phosphorylated-signal transducer and activator of transcription 1; MUC4, mucin 4; ZO-1, zonula occludens-1)

Figure 2. AMP-related gene expressions decreased along with downregulation of the p-STAT1/MUC4 complex in the ileum of EPEC-infected mice. (A/B/C/D/E/F/G). C57BL/6 mice were orally challenged with 100 μL of DMEM containing 10^{10} CFU/mL EPEC. (A). The expressions of p-STAT1 and MUC4 in the ileum were analyzed using Western blot, with GAPDH serving as the reference gene. (B/C/D/E/F). The expressions of Defa1, Defa4, Defa5, Camp and Lyz1 in the ileum were analyzed using qRT-PCR, with GAPDH serving as the reference gene. (G). In the ileum, the binding of STAT1 to MUC4 was examined by Co-Immunoprecipitation assay. $^{\#\#\#}P$ <0.001; $^{\#}$ compared the values of the connected two groups. (n=6). (EPEC, enteropathogenic Escherichia coli; p-STAT1, phosphorylated-signal transducer and activator of transcription 1; MUC4, mucin 4; AMP, antimicrobial peptide; qRT-PCR, quantitative reverse transcription polymerase chain reaction; DMEM, Dulbecco's modified eagle medium)

Figure 3. STAT1/MUC4 pathway was downregulated in EPEC-induced IEC and its forced upregulation resisted EPEC-induced IEC viability decrease. (A/B). The expressions of STAT1 and MUC4 in IECs transfected with STAT1 overexpression plasmids/NC or shMUC4/shNC were analyzed using qRT-PCR, with GAPDH serving as the reference gene. (C/D/E). IECs were transfected with NC plus shNC or STAT1 overexpression plasmids plus shNC/shMUC4, followed by EPEC (1×10^6 CFU/well) infection. (C/D). The expressions of STAT1 and MUC4 in the IECs were analyzed using qRT-PCR, with GAPDH serving as the reference gene. (E). The viability of the IECs was measured by cell counting kit-8 assay. $^{\#}P$ <0.05; $^{\#\#\#}P$ <0.001; $^{\#}$ compared

the values of the connected two groups. (n=3). (EPEC, enteropathogenic Escherichia coli; IEC, mouse intestinal epithelial cells; STAT1, signal transducer and activator of transcription 1; MUC4, mucin 4; shMUC4, short harpin RNA against MUC4; NC, negative control; shNC, short harpin RNA against negative control; qRT-PCR, quantitative reverse transcription polymerase chain reaction)

Figure 4. Forced upregulation of STAT1/MUC4 pathway offset EPEC-induced apoptosis promotion and release of proinflammatory cytokines in IEC. (A/B/C/D/E). IECs were transfected with NC plus shNC or STAT1 overexpression plasmids plus shNC/shMUC4, followed by EPEC (1×10^6 CFU/well) infection. (A/B). The apoptosis of the IECs was detected by flow cytometry. (C/D/E). The expressions of IL-1β, TNF-α and IL-6 in the IECs were analyzed using qRT-PCR, with GAPDH serving as the reference gene. $^{\#}P$ <0.05; $^{\#\#}P$ <0.001; $^{\#\#\#}P$ <0.001; $^{\#}$ compared the values of the connected two groups. (n=3). (EPEC, enteropathogenic Escherichia coli; IEC, mouse intestinal epithelial cells; IL-1β, interleukin-1β; TNF-α, tumor necrosis factor-α; IL-6, interleukin-6; STAT1, signal transducer and activator of transcription 1; MUC4, mucin 4; shMUC4, short harpin RNA against MUC4; NC, negative control; shNC, short harpin RNA against negative control; PI, propidium iodide; FITC, fluorescein isothiocyanate; qRT-PCR, quantitative reverse transcription polymerase chain reaction)

Figure 5. Forced upregulation of STAT1/MUC4 pathway resisted EPEC-induced ZO-1 downregulation in IEC. IECs were transfected with NC plus shNC or STAT1 overexpression plasmids plus shNC/shMUC4, followed by EPEC (1×10^6 CFU/well)

infection, and the expression of ZO-1 in the IECs was determined by immunofluorescence assay (magnification: × 400; scale bar: 50 μm). (n=3). (EPEC, enteropathogenic Escherichia coli; IEC, mouse intestinal epithelial cells; ZO-1, zonula occludens-1; STAT1, signal transducer and activator of transcription 1; MUC4, mucin 4; shMUC4, short harpin RNA against MUC4; NC, negative control; shNC, short harpin RNA against negative control; DAPI, 4',6-diamidino-2-phenylindole)

Figure 6. Forced upregulation of STAT1/MUC4 pathway reversed EPEC-induced AMP-related gene downregulation in IEC. (A/B/C/D/E). IECs were transfected with NC plus shNC or STAT1 overexpression plasmids plus shNC/shMUC4, followed by EPEC (1×10^6 CFU/well) infection, and the expressions of Defa1, Defa4, Defa5, Camp and Lyz1 in the ileum were analyzed using qRT-PCR, with GAPDH serving as the reference gene. $^{\#\#}P < 0.001$; $^{\#\#\#}P < 0.001$; $^{\#}$ compared the values of the connected two groups. (n=3). (EPEC, enteropathogenic Escherichia coli; IEC, mouse intestinal epithelial cells; STAT1, signal transducer and activator of transcription 1; MUC4, mucin 4; shMUC4, short harpin RNA against MUC4; NC, negative control; shNC, short harpin RNA against negative control; AMP, antimicrobial peptide; qRT-PCR, quantitative reverse transcription polymerase chain reaction)

Table

Table 1: Primers used in quantitative reverse transcription polymerase chain reaction for related genes

Genes	Species	Forward	Reverse
STAT1	mouse	5’-TCACAGTGGTTCGAGCTTCAG-3’	5’-GCAAACGAGACATCATAGGCA-3’
MUC4	mouse	5’-CCTCCTCTTGCTACCTGATGC-3’	5’-GGAACTTGGAGTATCCCTTGTTG-3’
IL-1β	mouse	5’-GCAACTGTTCCTGAACTCAACT-3’	5’-ATCTTTTGGGGTCCGTCAACT-3’
TNF-α	mouse	5’-CCCTCACACTCAGATCATCTTCT-3’	5’-GCTACGACGTGGGCTACAG-3’
IL-6	mouse	5’-TAGTCCTTCCTACCCCAATTTCC-3’	5’-TTGGTCCTTAGCCACTCCTTC-3’
Defa1	mouse	5’-AGAAGAGGACCAGGCCGTAT-3’	5’-GAAGTGCCTTCTGGGTCTCC-3’
Defa4	mouse	5’-GAGTTCGTGGGACTTGTGGA-3’	5’-CATCTGCATGTTCAGCGGC-3’

Defa5	mouse	5’-TGGATGCTTGCAGTCTCCTG-3’	5’-GCCAAGGGAGCCACATTACT-3’
Lyz1	mouse	5’-GAGACCGAAGCACCGACTATG-3’	5’-CGGTTTTGACATTGTGTTCGC-3’
GAPDH	mouse	5’-AGGTCGGTGTGAACGGATTTG-3’	5’-TGTAGACCATGTAGTTGAGGTCA-3’

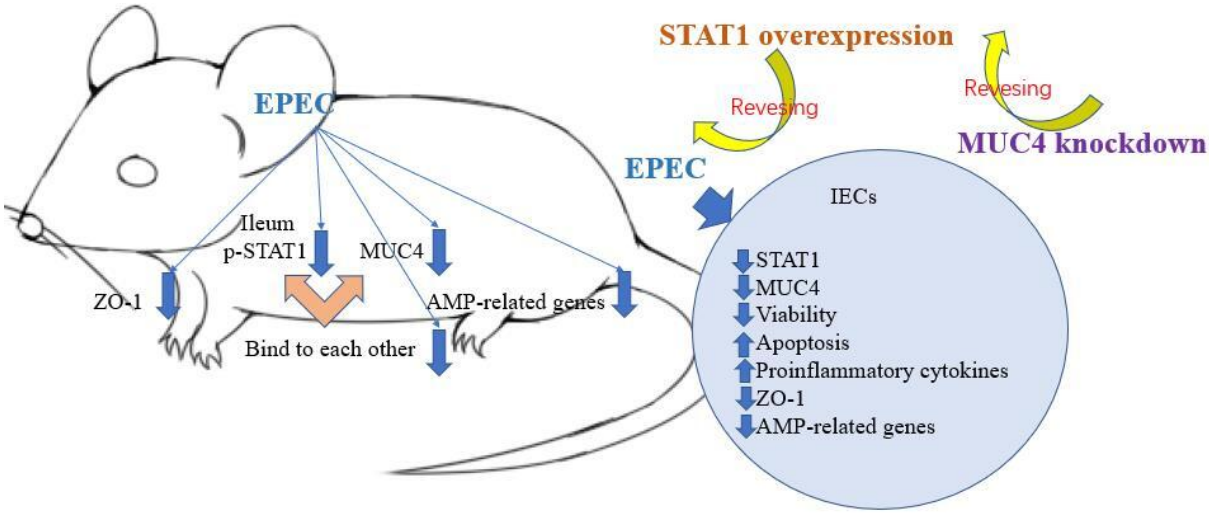
STAT1 overexpression
Revesing
Revesing
MUC4 knockdown
EPEC
EPEC
IECs
Ileum
p-STAT1
MUC4
ZO-1
AMP-related genes
Bind to each other
STAT1
MUC4
Viability
Apoptosis
Proinflammatory cytokines
ZO-1
AMP-related genes

Table 1: Primers used in quantitative reverse transcription polymerase chain reaction for related genes

Genes	Species	Forward	Reverse
STAT1	mouse	5’-TCACAGTGGTTCGAGCTTCAG-3’	5’-GCAAACGAGACATCATAGGCA-3’
MUC4	mouse	5’-CCTCCTCTTGCTACCTGATGC-3’	5’-GGAACTTGGAGTATCCCTTGTTG-3’
IL-1β	mouse	5’-GCAACTGTTCCTGAACTCAACT-3’	5’-ATCTTTTGGGGTCCGTCAACT-3’
TNF-α	mouse	5’-CCCTCACACTCAGATCATCTTCT-3’	5’-GCTACGACGTGGGCTACAG-3’
IL-6	mouse	5’-TAGTCCTTCCTACCCCAATTTCC-3’	5’-TTGGTCCTTAGCCACTCCTTC-3’
Defa1	mouse	5’-AGAAGAGGACCAGGCCGTAT-3’	5’-GAAGTGCCTTCTGGGTCTCC-3’
Defa4	mouse	5’-GAGTTCGTGGGACTTGTGGA-3’	5’-CATCTGCATGTTCAGCGGC-3’
Defa5	mouse	5’-TGGATGCTTGCAGTCTCCTG-3’	5’-GCCAAGGGAGCCACATTACT-3’
Lyz1	mouse	5’-GAGACCGAAGCACCGACTATG-3’	5’-CGGTTTTGACATTGTGTTCGC-3’
GAPDH	mouse	5’-AGGTCGGTGTGAACGGATTTG-3’	5’-TGTAGACCATGTAGTTGAGGTCA-3’

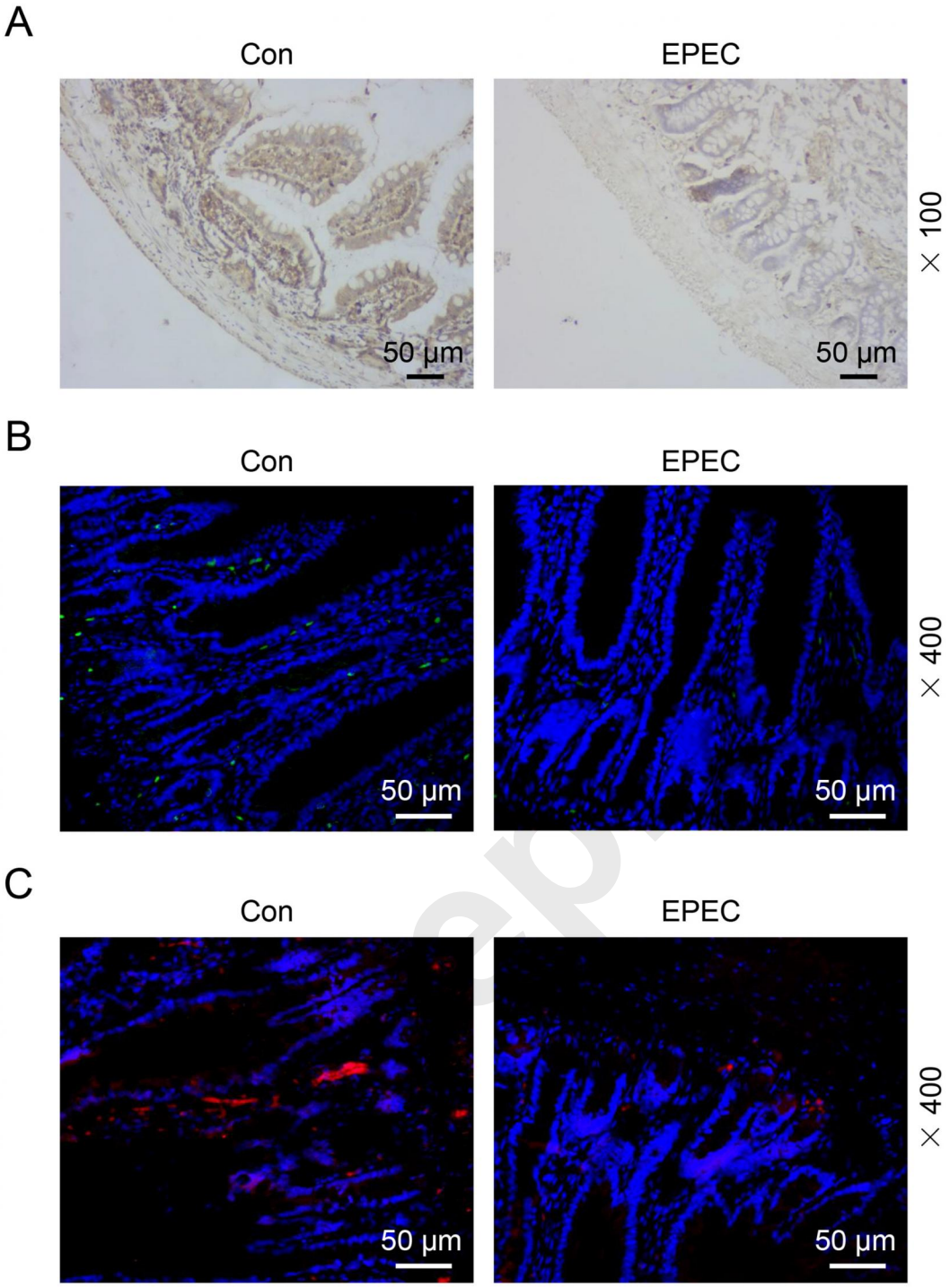
A
Con
EPEC
50 μm
50 μm
× 100
B
Con
EPEC
50 μm
50 μm
× 400
C
Con
EPEC
50 μm
50 μm
× 400

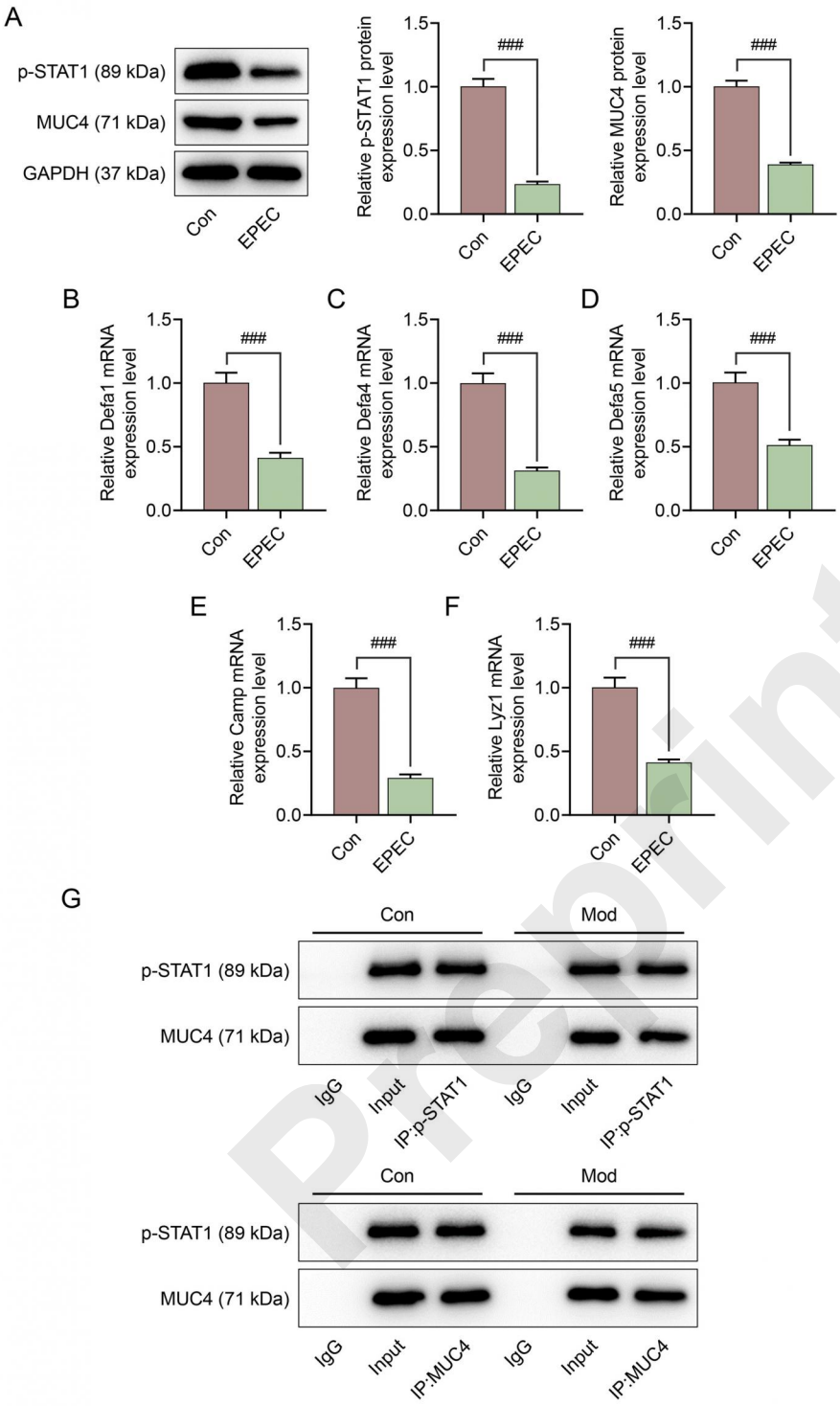
A
p-STAT1 (89 kDa)
MUC4 (71 kDa)
GAPDH (37 kDa)
Con
EPEC
Relative p-STAT1 protein expression level
Relative MUC4 protein expression level
###
1.5
1.0
0.5
0.0
B
Relative Defa1 mRNA expression level
C
Relative Defa4 mRNA expression level
D
Relative Defa5 mRNA expression level
E
Relative Camp mRNA expression level
F
Relative Lyz1 mRNA expression level
G
Con
Mod
p-STAT1 (89 kDa)
MUC4 (71 kDa)
IgG
Input
IP:p-STAT1
IP:MUC4

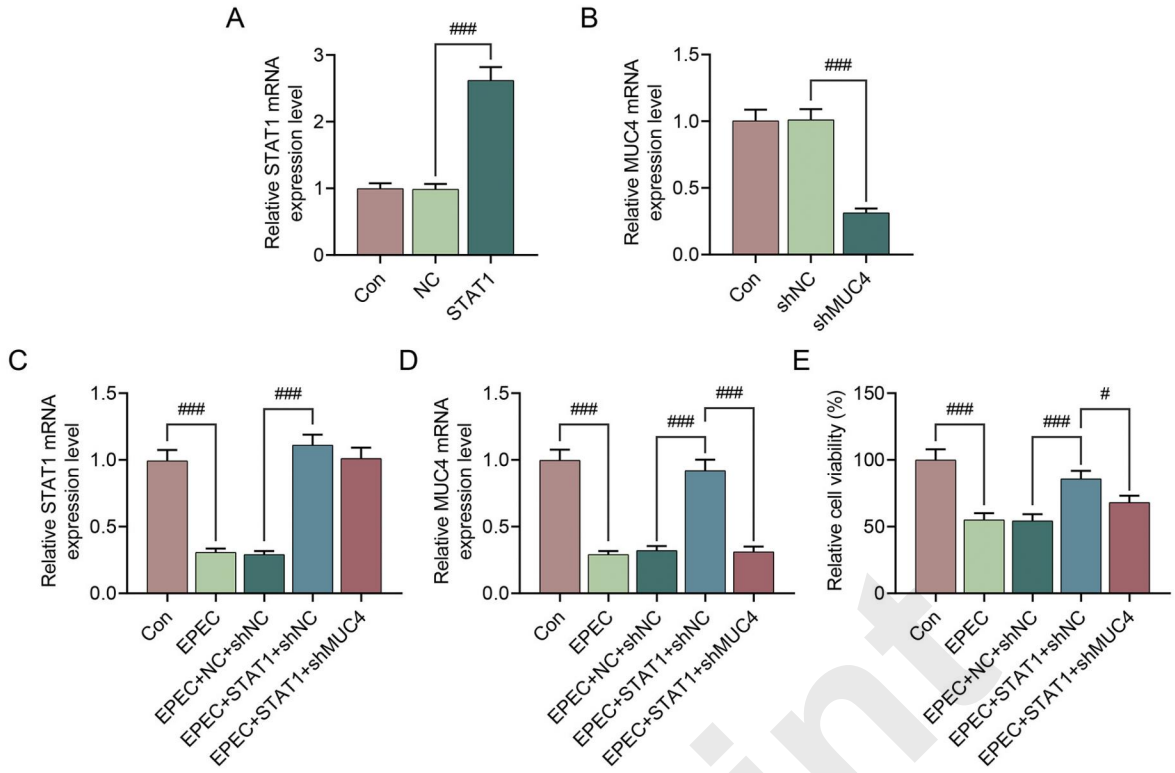
A
Relative STAT1 mRNA expression level
###
Con
NC
STAT1
B
Relative MUC4 mRNA expression level
###
Con
shNC
shMUC4
C
Relative STAT1 mRNA expression level
###
###
Con
EPEC
EPEC+NC+shNC
EPEC+STAT1+shNC
EPEC+STAT1+shMUC4
D
Relative MUC4 mRNA expression level
###
###
###
Con
EPEC
EPEC+NC+shNC
EPEC+STAT1+shNC
EPEC+STAT1+shMUC4
E
Relative cell viability (%)
###
###
#
Con
EPEC
EPEC+NC+shNC
EPEC+STAT1+shNC
EPEC+STAT1+shMUC4

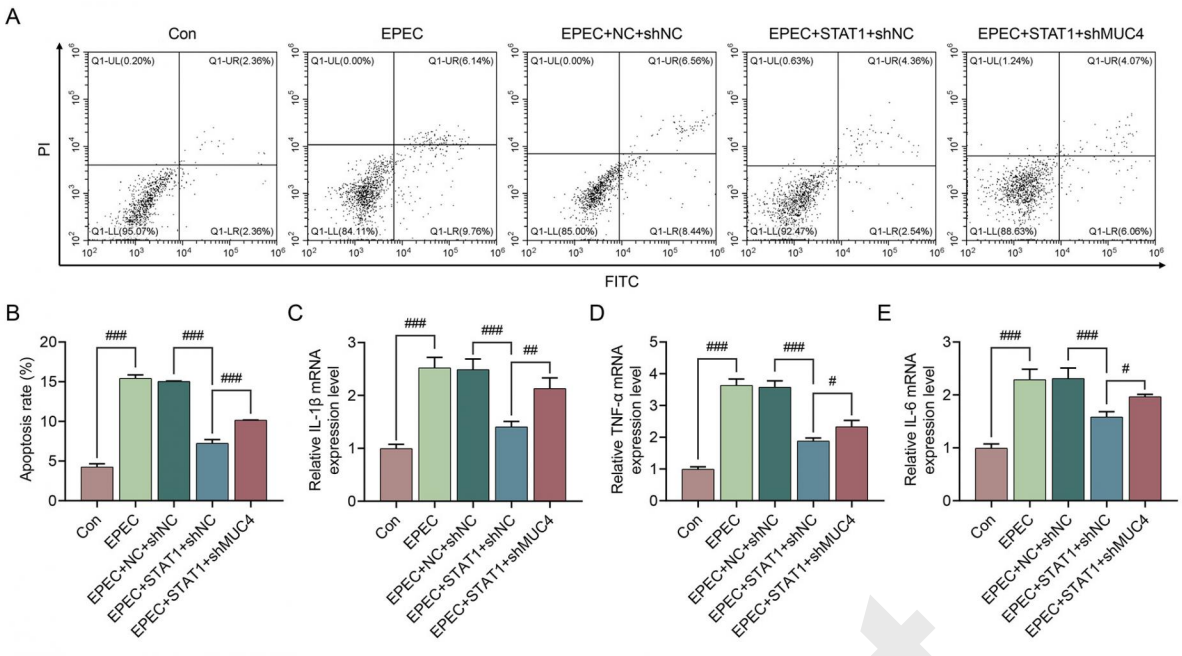
A
Con
EPEC
EPEC+NC+shNC
EPEC+STAT1+shNC
EPEC+STAT1+shMUC4
PI
FITC
Q1-UL(0.20%)
Q1-UR(2.36%)
Q1-LL(95.07%)
Q1-LR(2.36%)
Q1-UL(0.00%)
Q1-UR(6.14%)
Q1-LL(84.11%)
Q1-LR(9.76%)
Q1-UL(0.00%)
Q1-UR(6.56%)
Q1-LL(85.00%)
Q1-LR(8.44%)
Q1-UL(0.63%)
Q1-UR(4.36%)
Q1-LL(92.47%)
Q1-LR(2.54%)
Q1-UL(1.24%)
Q1-UR(4.07%)
Q1-LL(88.63%)
Q1-LR(6.06%)
B
Apoptosis rate (%)
C
Relative IL-1β mRNA expression level
D
Relative TNF-α mRNA expression level
E
Relative IL-6 mRNA expression level
###
##
#
Con
EPEC
EPEC+NC+shNC
EPEC+STAT1+shNC
EPEC+STAT1+shMUC4

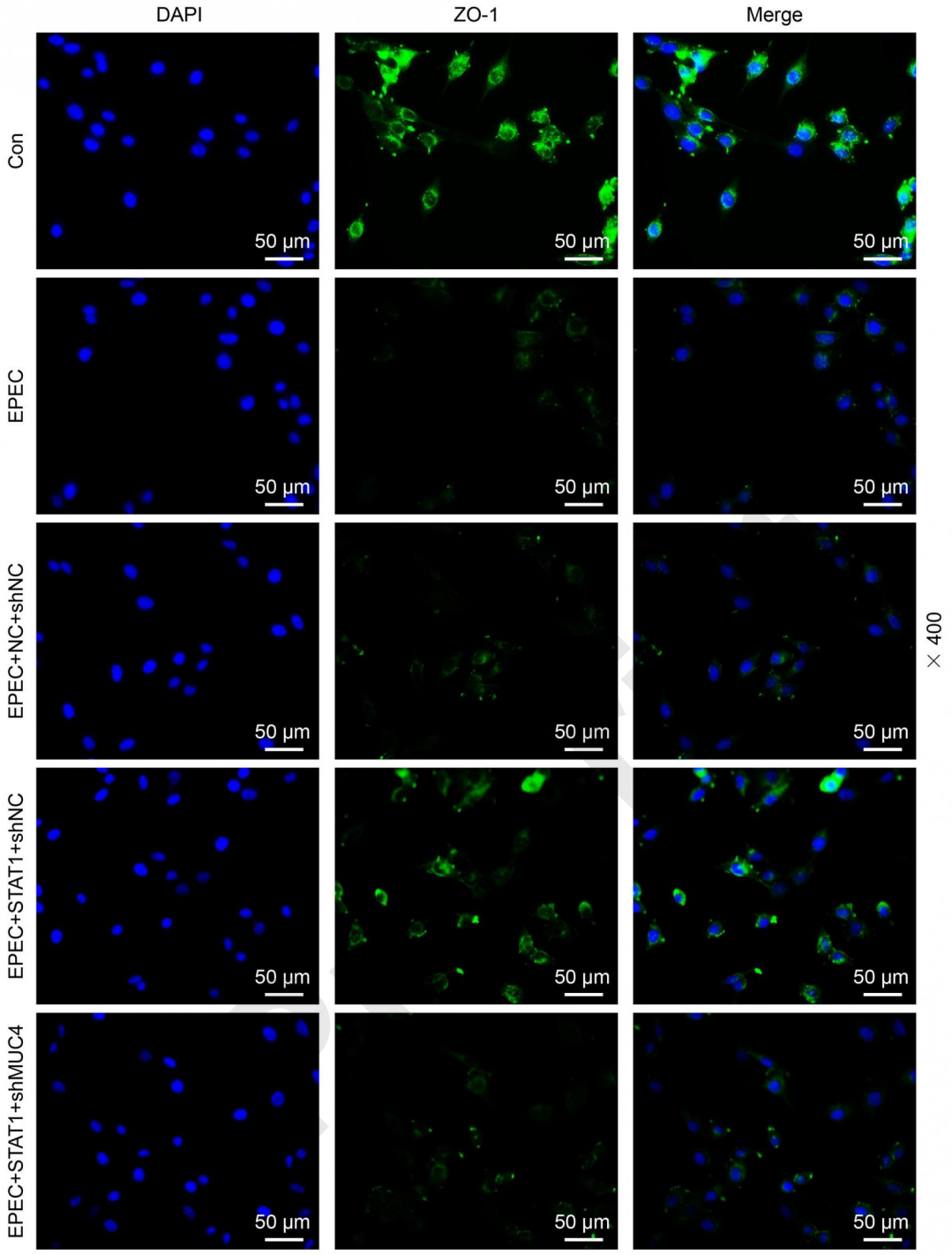
DAPI
ZO-1
Merge
Con
EPEC
EPEC+NC+shNC
EPEC+STAT1+shNC
EPEC+STAT1+shMUC4
50 μm
× 400

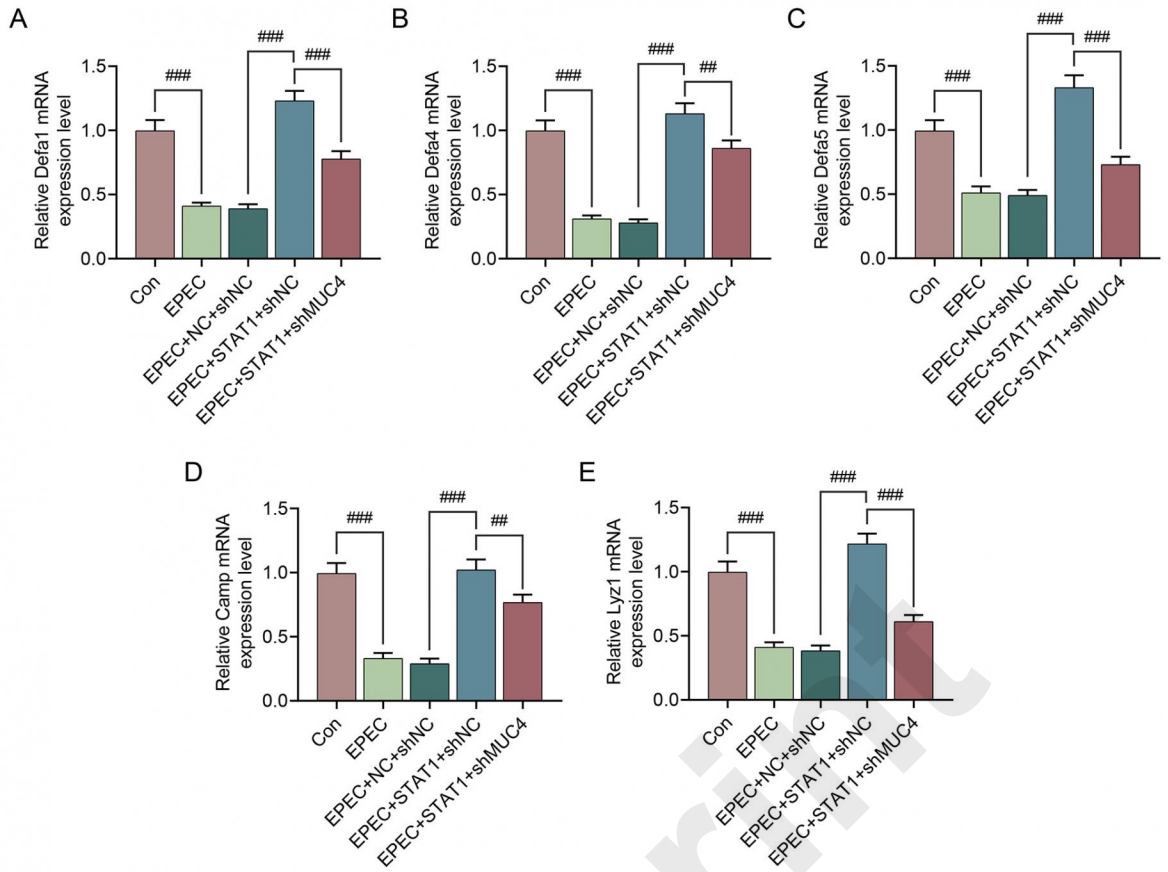
A
Relative Defa1 mRNA expression level
1.5
1.0
0.5
0.0
###
###
###
Con
EPEC
EPEC+NC+shNC
EPEC+STAT1+shNC
EPEC+STAT1+shMUC4
B
Relative Defa4 mRNA expression level
###
###
##
C
Relative Defa5 mRNA expression level
###
###
###
D
Relative Camp mRNA expression level
###
###
##
E
Relative Lyz1 mRNA expression level
###
###
###